ELSEVIER

Precambrian Research 00 (2002) 1–18

Precambrian Research

www.elsevier.com/locate/precamres

Late Proterozoic magmatism and metamorphism recorded in gneisses from the Dabie high-pressure metamorphic zone, eastern China: evidence from zircon U–Pb geochronology

Fukun Chen[a,b,*], Wolfgang Siebel[b], Jinghui Guo[a], Bolin Cong[a], Muharrem Satir[b]

[a] *Institute of Geology and Geophysics, Chinese Academy of Sciences, P.O. Box 9825, Beijing 100029, China*
[b] *Institut für Geowissenschaften, Universität Tübingen, Wilhelmstraße 56, 72074 Tubingen, Germany*

Received 8 February 2002; received in revised form 28 September 2002; accepted 30 September 2002

Abstract

This study presents zircon ages and geochemical and Nd-isotopic data for metagranites and quartzites from the Susong high-pressure metamorphic zone in the Dabie–Sulu ultrahigh-pressure collisional belt. This belt belongs to the eastern part of the Qinling–Dabie orogenic belt that formed during Early Mesozoic collision of the North and South China Blocks. Two metagranites give zircon U–Pb model ages of 785±7 and 205±12 Ma, likely representing a Late Proterozoic magmatic event and an Early Mesozoic overprint. They have low initial ε_{Nd}-values (−12.4 and −11.1 at 780 Ma), favouring a crustal origin. Flat heavy rare earth elements (REE) patterns ($Gd_N/Yb_N \sim 1.2$) probably reflect that melting took place at a shallow crustal section where heavy-REE-bearing mineral phases are unstable. All zircons of three quartzites yield young discordant U–Pb ages and define a discordia with U–Pb model ages of 784±6 and 213±3 Ma, identical to those of the metagranites. We assume that all detrital zircons had lost radiogenic Pb prior to the Early Mesozoic overprint, probably facilitated by fluid participation during a metamorphic event contemporaneous with the intrusion of the metagranites. This simultaneous metamorphic and magmatic event was probably related to a rift setting along the periphery of the Yangtze (South China) Block during Late Proterozoic.

Keywords: Dabie; Late Proterozoic; Magmatism; Metamorphism; Zircon U–Pb age

1. Introduction

The Dabie–Sulu terrain represents the eastern part of the Qinling–Dabie orogenic belt that resulted from the collision between the Yangtze (South China) and North China (Sino-Korean)

* Corresponding author
E-mail addresses: fukun.chen@uni-tuebingen.de, cfk@btamail.net.cn (F. Chen).

0301-9268/02/$ - see front matter © 2002 Published by Elsevier Science B.V.
PII: S0301-9268(02)00162-6

Blocks and possible intervening microplates (e.g. Klimetz, 1983; Liu and Hao, 1989; Ma, 1989; Zhang, 1997; Meng and Zhang, 2000). Numerous structural and tectonic models have been proposed to interpret the orogenic processes that built up this huge belt (e.g. Mattauer et al., 1985; Hsü et al., 1987; Ma, 1989; Huang and Wu, 1992; Yin and Nie, 1993; Lee et al., 1997b; Meng and Zhang, 2000). Radiometric data achieved in recent years favour an Early Mesozoic collision (e.g. Mattauer et al., 1991; Li et al., 1993, 2000; Ames et al., 1993; Eide et al., 1994; Cong et al., 1995). This corresponds to the change from marine to continental sedimentation in the Yangtze block (e.g. Enkin et al., 1992).

In the Dabie area, numerous radiometric studies were carried out on rocks associated with the ultrahigh-pressure (UHP) metamorphism to constrain the collision time and the exhumation of the UHP rocks (e.g. Li et al., 1993; Eide et al., 1994; Hacker et al., 1995, 1998; Hacker and Wang, 1995; Ames et al., 1996; Chavagnac and Jahn, 1996; Xue et al., 1997; Rowley et al., 1997; Xu et al., 2000; Chavagnac et al., 2001). A part from numerous ages around 220–230 Ma that date the collision time, several chronological studies, especially U–Pb zircon dating demonstrate that at least three events at around 450 Ma, 700–800 Ma, and > 1000 Ma are recorded in various metamorphic rocks from the Dabie Mountains (e.g. Ames et al., 1996; Rowley et al., 1997; Hacker et al., 1998; Xie et al., 2001). A U–Pb upper-intercept age of 447 Ma of zircons from an UHP eclogite near Maowu was considered to represent the age of crystallisation of the protolith (Rowley et al., 1997). Similar ages have been also obtained on an orthogneiss from the South Dabie zone and an amphibolite and schist from the Susong high-pressure (HP) metamorphic zone (Xie et al., 2001). Although similar magmatic and metamorphic ages were reported in the western part of the Qinling–Dabie belt (e.g. Kröner et al., 1993; Lerch et al., 1995; Xue et al., 1996) and interpreted as reflecting Siluro-Devonian metamorphism accompanying arc magmatism (Zhai et al., 1998), it is somewhat problematic to interpret the Early Palaeozoic ages for the Dabie area however. Nevertheless, the majority of zircon U–Pb upper-intercept ages reported in previous studies from UHP eclogites and orthogneisses of the Dabie–Sulu area range about from 700 to 800 Ma (e.g. Ames et al., 1993; Rowley et al., 1997; Xue et al., 1997; Hacker et al., 1998; Chavagnac et al., 2001). These ages are commonly considered as crystallisation ages of protoliths of the eclogites and are related to an extension environment (e.g. Ames et al., 1996). In contrast, geochronological studies on other metamorphic zones of the Dabie–Sulu terrain are less performed heretofore. Consequently, the evolution of the basements within this orogenic belt prior to the Early Mesozoic collision has been less recognized. Here we present radiometric data for gneisses of the Susong zone to reveal an earlier magmatic and metamorphic history. We observe that zircons from both ortho- and para-gneisses give U–Pb model ages clustering at about 780 Ma. This phenomenon is interpreted as evidence for a contemporaneous Late Proterozoic magmatic-metamorphic event along the northern margin of the Yangtze block, which probably was related to the break-up of the Late Proterozoic supercontinent, Rodinia.

2. Geological background

The Dabie terrain is made up of several major tectonically juxtaposed units, i.e. from north to south, the Beihuaiyang low-grade metamorphic zone, the North Dabie gneiss zone (dome unit; Hacker et al., 1995), the South Dabie UHP metamorphic zone, and the Susong HP metamorphic zone (Fig. 1). It is bounded to the north by the basement of the North China Block, which is covered by Mesozoic volcano-sedimentary rocks, and to the south by the Yangtze foreland fold and thrust belt that is composed mainly of Palaeozoic to Triassic clastic and carbonate strata (Liou et al., 1995). Cretaceous post-collisional granitoids intrude into all the major zones (Ma et al., 1998).

The Susong HP metamorphic zone comprises metamorphosed quartz sandstone, schist, marble, biotite gneiss, quartz-rich amphibolite and metaphosphorite (Liou et al., 1995). This zone is also known as the South Dabie HP unit (e.g. Carswell

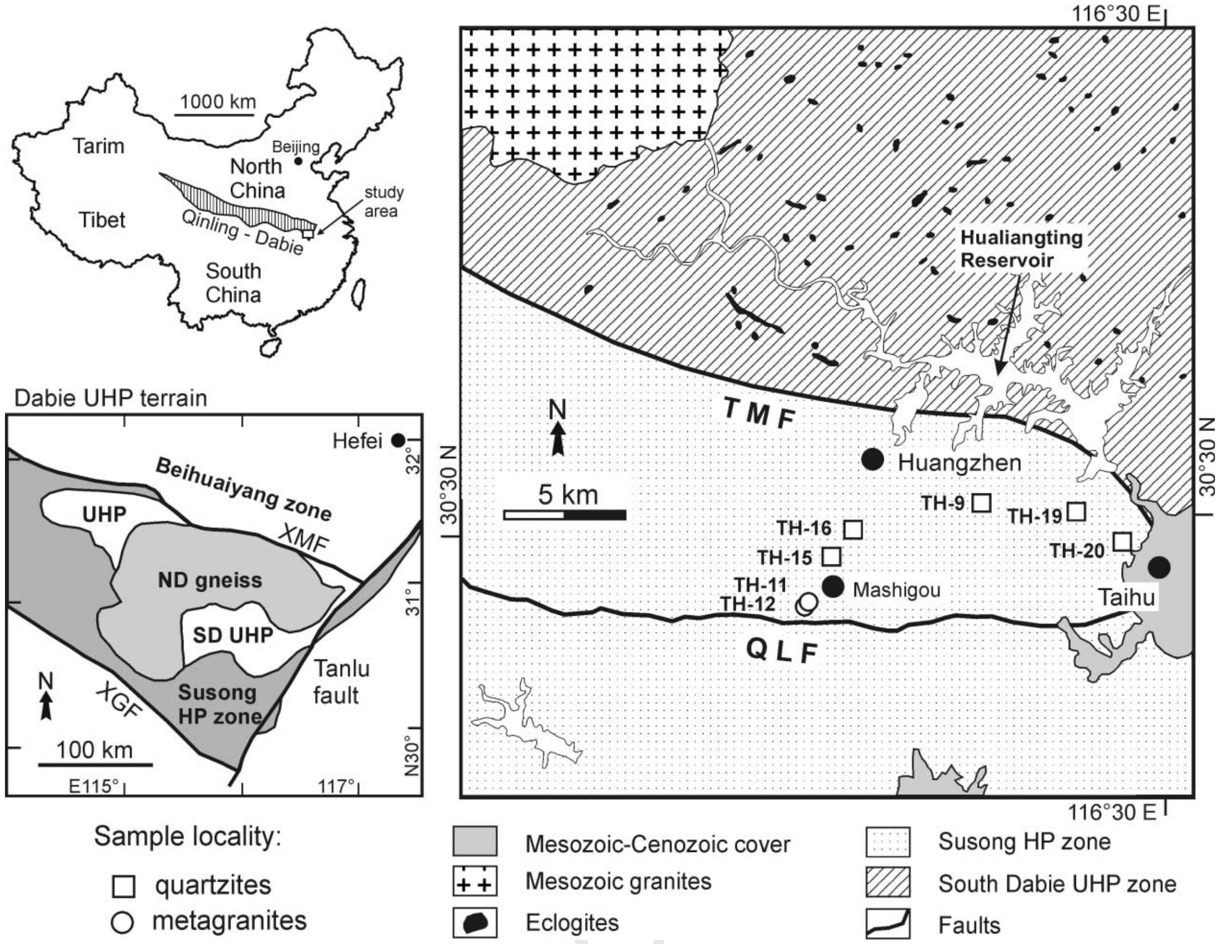

Fig. 1. Simplified geological map of the study area (e.g. AGS, 1999; Liou et al., 1995; Hacker et al., 1998). *Abbreviations:* ND, North Dabie; SD, South Dabie; UHP, ultrahigh-pressure; HP, high-pressure; XMF, the Xiaotian-Mozitan fault; TMF, the Taihu-Mamiao fault; QLF, the Queyueling-Longshan fault; XGF, the Xiangfan-Guangji fault.

et al., 1997) or the *Susong Metamorphic Complex* (e.g. Liou et al., 1995). The southern boundary of the Susong zone is marked by the Xiangfan-Guangji fault (e.g. Liou et al., 1995; Dong et al., 1998). Whether the northern boundary is marked by the Taihu-Mamiao fault or the Queyueling-Longshan fault is still discussed. As the same rock suite can be observed on both sides of the Queyueling-Longshan fault, it is suggested that the boundary of the Susong HP zone and the South Dabie UHP zone extends from the north of Huangzhen eastward through the dam of the Hualiangting reservoir (Zhai et al., 1995). The rock assemblage between the two faults, mainly quartz schists and quartzites, has also been defined as the *Dabie Schist Group* (e.g. AGS, 1999) and regarded as part of the *Dabie Formation* or the *Dabie Metamorphic Complex*. The rock sequences south of the Queyueling-Longshan fault are defined as the *Susong Formation*, which contains a characteristic phosphorite-bearing metamorphic sequence.

Within the Susong zone, metamorphic grade in general changes southwards from amphibolite-eclogite-facies through amphibolite-facies to greenschist-facies. Based on the different metamorphic conditions, the Susong zone was further subdivided into three units (Liou et al., 1995). Estimated metamorphic temperatures vary from ~500 °C in the northern unit, ~430 °C in the central unit, to ~300 °C in the southern unit (Liou et al., 1995). The northern unit is composed of thick metamorphosed magnetite-bearing quartz sandstone with thin layers of mica schist and granitic gneiss. Lenses of quartz eclogite occur within the sandstone along the northern margin. These eclogites underwent metamorphism under conditions of ~600–635 °C and 18 kbar and were referred to as *cold eclogites* that are different from the *hot eclogites* exposed in the South Dabie UHP zone (Okay, 1993). The central unit comprises magnetite-bearing quartz sandstone, marble, quartzite, garnet-biotite gneiss, quartz hornblendite, metaphosphorite, and kyanite-bearing quartzite, interlayered with each other. The dominant rocks in the southern unit are chlorite–sericite schist, greenschist, and fine-grained biotite gneiss.

In contrast to the South Dabie UHP zone, geochronological investigations of rocks from the Susong zone are still in a reconnaissance stage. Xie et al. (2001) reported zircon U–Pb ages of a schist and amphibolite sample, south of the Queyueling-Longshan fault. Intercept ages of the schist are 401±24 and 1164±210 Ma and three zircon fractions from the amphibolite give $^{206}Pb/^{238}U$ ages ranging from ~450 to ~2400 Ma. Two Rb–Sr ages of 844±73 Ma (whole-rock isochron) and 231±48 Ma (whole-rock/phengite isochron) as well as a K–Ar phengite age of 211 Ma were reported for metamorphic rocks from the south-eastern part of this zone (Sang et al., 1987).

3. Analytical methods

Whole-rock powder was obtained by crushing and splitting about 5–10 kg of samples. Zircons were separated from the crushed rocks using a shaking table, a Frantz isodynamic separator and heavy liquids and finally handpicked under a binocular microscope. Zircon grains studied by cathodoluminescence (CL) investigation were mounted in epoxy resin and polished down to expose grain centres. The CL images were obtained using a microprobe JEOL JXA-8900RL at the University of Tübingen, working at 15 kV. Major and trace element concentrations of whole-rock samples were analysed on fused glass discs by X-ray fluorescence spectrometry (XRF) at University of Tübingen. Loss of ignition (LOI) was determined after igniting sample powder at 1000 °C for 1 h. Concentrations of rare earth elements (REE) and selected trace elements were determined by ICP-mass spectrometry (ICP-MS) at Memorial University, St. John's, Newfoundland, using the HF–HNO_3 digestion of sample powder and the analytical methods within the precision and accuracy described by Jenner et al. (1990). The ICP-MS and XRF data on the elements of Rb, Sr, Ba, Y, Zr, and Nb as well as the ICP-MS and isotope dilution data on the elements of Sm and Nd were used to check the dissolution procedure.

For Nd and Sm isotope analyses, light REE (LREE) were isolated on quartz columns by conventional ion exchange chromatography with a 5-ml resin bed of AG 50W-X12 (200–400 mesh) and Sm and Nd were separated from each other and other REE on quartz columns using 1.7-ml Teflon powder as cation exchange medium. For U–Pb analyses, single zircons or populations consisting of two to three morphologically identical grains were mechanically abraded following the Krogh method (1982). After the abrasion, they were washed shortly in warm 7 N HNO_3 and warm 6 N HCl, prior to dissolution to remove surface contamination. Then, a mixed ^{205}Pb–^{235}U-tracer solution was added to the grain. Dissolution was performed in PTFE vessels in a Parr digestion bomb (Parrish, 1987) at 200 °C for 7 days in 22 N HF and for 1 day in 6 N HCl to assure re-dissolution of the fluorides into chloride salts. Separation and purification of U and Pb were carried out on Teflon columns with a 40-μl bed of AG1-X8 (100–200 mesh) anion exchange resin. The technique used for single zircon Pb evaporation is that developed by Kober (1986). The Pb isotopes were dynamically measured in a sequence of 206-207-208-204-206-207 with a secondary electron multiplier. Common lead correction followed Cocherie et al. (1992). The calculated $^{207}Pb/^{206}Pb$ ages are based on the means of all measurements evaluated and the errors are given in 2σ standard deviation. Further details on the analytical techniques are given in Chen et al. (2000, 2002).

All isotopic measurements were made on a Finnigan MAT 262 mass spectrometer at the University of Tübingen. Sm and Nd were loaded on Re-filaments and measurements were performed in a double-filament configuration. $^{143}Nd/^{144}Nd$ ratios were normalised to $^{146}Nd/^{144}Nd$ ratio of 0.7219. Analyses of the Ames metal gave a $^{143}Nd/^{144}Nd$ ratio of 0.512125 ± 0.000010 ($n = 24$), close to the reference value of 0.512147 ± 0.000007 (Roddick et al., 1992). Measured $^{143}Nd/^{144}Nd$ ratios of samples were normalised to this reference value. Total procedural blanks were < 50 pg for Sm and Nd. Pb was loaded with a Si-gel onto a Re-filament and measured at ~ 1300 °C in a single-filament configuration, while U was loaded with 1N HNO_3 onto a Re-filament and measured in a double-filament configuration. Total procedural Pb and U blanks were < 10 pg. A factor of 1‰ per atomic mass unit for instrumental mass fractionation was applied to all Pb analyses, using NBS 981 as reference material. Initial common Pb remaining after correction for tracer and blank was corrected using values from the Stacey and Kramers (1975) model. The U–Pb data were evaluated with the *Pbdat* program (Ludwig, 1988) and regression of U–Pb discordia was done following the regression treatment of Wendt (1986). All errors are given as $2\sigma_m$. Repeated measurements on zircon standard 91 500 gave nearly concordant U–Pb ages of 1065.6 ± 2.2 Ma (Chen et al., in press), consistent with the U–Pb age of 1065.4 ± 0.3 Ma obtained in different laboratories (Wiedenbeck et al., 1995). The Pb evaporation analyses on zircon 91 500 and Phalaborwa zircon (South Africa) yielded $^{207}Pb/^{206}Pb$ ages of 1063 ± 5 and 2054.1 ± 0.5 Ma, respectively, consistent with the reported values (Wiedenbeck et al., 1995; Kröner et al., 1993).

4. Samples and analytical results

4.1. Samples

Analysed samples were collected from the northern part of the Susong zone (Fig. 1). Rocks from this part were subjected to amphibolite-facies metamorphism. Two metagranite samples TH-11 and TH-12 were collected along a new road near the Mashigou village. Both samples are leucocratic, foliated, homogeneously medium-grained and consist of quartz, feldspar, biotite, muscovite and accessory apatite and zircon. Sample TH-9 is a light grey, foliated quartzite and contains $> 50\%$ quartz, $> 20\%$ feldspar, about 5% magnetite, and about 5% muscovite and chlorite. Samples TH-15, TH-16, TH-19, and TH-20 are light grey or green to pink, slightly to strongly foliated quartzites, which are composed of about 70% quartz, 10% feldspar, 5–10% muscovite, and 2–5% magnetite. All the quartzites contain zircon and apatite as accessory phases.

4.2. Geochemical composition

Major and trace element concentrations of whole-rock samples are given in Table 1. Normalised concentrations of REE and other trace elements of two metagranite (TH-11 and TH-12) and two quartzite (TH-16 and TH-19) samples are shown in Fig. 2. The metagranites are plotted in the monzogranite field in a quartz-plagioclase-K-feldspar diagram (LeMaitre, 1989), according to their modal compositions. They contain about 76 wt.% SiO_2 and 8.1–8.7 wt.% ($K_2O + Na_2O$) and have K_2O/Na_2O ratios of 1.3–1.4 and A/CNK ratios of about 1.1 (mole $Al_2O_3/(CaO + Na_2O + K_2O)$). Five quartzite samples contain about 76–78 wt.% SiO_2 and 6.3–8.0 wt.% ($K_2O + Na_2O$). They have variable K_2O/Na_2O ratios ranging from about 0.6 to 1.8.

Two analysed metagranite samples similarly have a steep LREE and flat heavy REE (HREE) pattern, as expressed by La_N/Yb_N ratios of 6.5–8.2 and Gd_N/Yb_N ratios of about 1.2, when normalised to chondrite (Fig. 2a). They also exhibit a strong negative Eu-anomaly (Eu/Eu* ~ 0.11–0.24; $Eu^* = (Sm_N \times Gd_N)^{1/2}$), which can indicate

Table 1
Whole-rock major and trace element concentrations of metagranites and quartzites from the Susong HP metamorphic zone

Sample	TH-11 metagranite	TH-12 metagranite	TH-16 quartzite	TH-19 quartzite	TH-9 quartzite	TH-15 quartzite	TH-20 quartzite
SiO_2	75.4	75.5	76.3	76.9	75.9	77.7	77.7
TiO_2	0.16	0.11	0.16	0.13	0.20	0.16	0.17
Al_2O_3	13.29	12.58	12.94	12.14	10.44	11.94	12.12
Fe_2O_3	1.28	1.18	2.04	2.01	2.99	1.17	1.49
MnO	0.03	0.04	0.03	0.03	0.06	0.02	0.01
MgO	0.06	b.d.	b.d.	b.d.	0.25	b.d.	b.d.
CaO	0.65	0.27	0.09	0.24	1.01	0.14	0.13
Na_2O	3.60	3.46	2.52	4.34	3.89	3.11	2.90
K_2O	5.06	4.60	4.54	3.62	2.41	4.91	4.94
P_2O_5	0.03	0.01	0.02	0.01	0.02	0.02	0.01
LOI	0.38	0.32	1.14	0.29	1.82	0.27	0.64
Total	100.04	98.13	99.91	99.88	99.17	99.65	100.19
A/CNK	1.06	1.13	1.40	1.06	0.96	1.12	1.17
Ba	408	526	478	788	1192	1226	111
Cr	7	b.d.	10	5	b.d.	2	85
Nb	14	24	53	16	16	12	22
Rb	197	193	183	60	45	116	117
Sr	58	30	17	35	89	40	8
Y	34	31	31	50	50	40	58
Zr	145	122	400	391	644	174	456
Ta	2.0	2.8	4.1	1.2			
Cs	2.8	1.5	4.0	0.6			
Pb	23.0	23.9	20.9	13.5			
Th	23.5	20.0	21.8	9.5			
U	2.3	2.1	4.2	0.6			
La	41.7	37.1	78.2	65.4			
Ce	71.4	62.1	123.4	140.2			
Pr	9.0	6.7	22.1	11.9			
Nd	28.2	28.9	62.6	54.3			
Sm	5.2	6.5	12.5	10.9			
Eu	0.4	0.2	1.0	1.2			
Gd	5.1	5.7	11.7	9.0			
Tb	0.8	1.0	1.3	1.6			
Dy	5.3	5.6	6.6	8.7			
Ho	1.1	1.3	1.1	2.0			
Er	3.2	3.2	3.6	5.9			
Tm	0.5	0.6	0.5	0.9			
Yb	3.4	3.8	3.0	5.8			
Lu	0.4	0.4	0.4	0.7			
$(La/Yb)_N$	8.2	6.5	17.5	7.6			
$(Gd/Yb)_N$	1.2	1.2	3.1	1.2			
Eu/Eu*	0.24	0.11	0.08	0.37			
$^{147}Sm/^{144}Nd$	0.1146	0.1462	0.1158	0.1194	0.1189	0.1241	0.1089
$^{143}Nd/^{144}Nd$	0.511584	0.511810	0.511916	0.511916	0.511840	0.511927	0.511690
$\varepsilon_{Nd}(t)$	−12.4	−11.1	−6.0	−6.4	−7.4	−6.6	−9.7
T_{DM} (Ga)	2.4	2.3	1.9	1.9	2.0	1.9	2.2

b.d., Below detection limit. Major and trace element concentrations in wt.% and ppm, respectively. A/CNK = mole $Al_2O_3/(CaO+Na_2O+K_2O)$. Errors of the measured $^{143}Nd/^{144}Nd$ ratios are $<1.2\times10^{-5}$. Initial ε_{Nd} values are calculated for $t=780$ Ma. T_{DM} values are calculated assuming a two-stage model of Liew and Hofmann (1988).

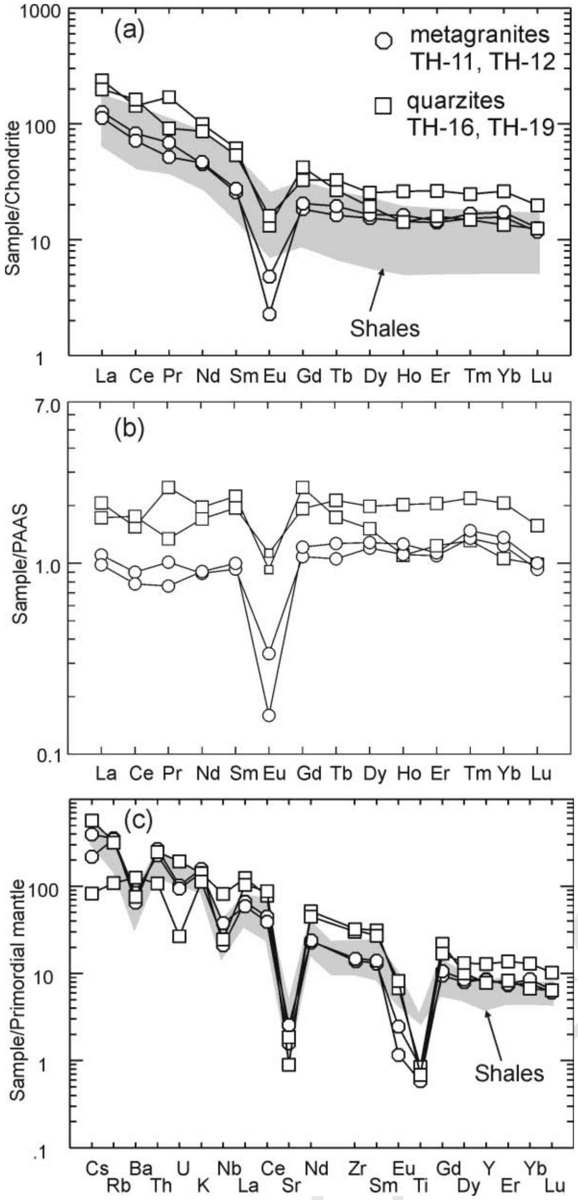

Fig. 2. Normalized trace element concentrations of metagranites and quartzites. Normalizing values for chondrite, primordial mantle, and PAAS are from Sun (1982), Taylor and McLennan (1985), and McLennan (1989), respectively. Literature data for shales: Nance and Taylor (1976).

fractionation of plagioclase from the melt(s) and/or inheritance from the source material. The REE patterns of two quartzites (TH-16 and TH-19) are similar to those of the metagranites, but they have higher REE-contents. These two quartzite samples are further different from each other in the HREE-contents. When all four samples are normalised to the Post-Archaean average Australian sedimentary rocks (PAAS) (McLennan, 1989), the difference between the metagranites and quartzites becomes more evident. The two metagranites show a slight HREE enrichment but have similar LREE-contents, compared to the PAAS (Fig. 2b). Trace element concentrations normalised to the primordial mantle show both the metagranites and quartzites distinctly have negative anomalies of Nb, Sr, and Ti, which can be observed in rocks having a crustal origin. The metagranites have similar patterns of normalised trace element compositions, while these two quartzite samples differ from each other in Rb-, Ba-, and U-contents as well as in HREE concentrations.

4.3. Zircon internal structure and ages

Internal structure of zircons was studied with the CL technique, which allows an examination of magmatic zoning, inherited xenocryst, and overgrowth in zircon grains (e.g. Hanchar and Miller, 1993). About 60 zircon grains from the metagranites (TH-11 and TH-12) and the quartzites (TH-16 and TH-19) were studied and the CL images shown in Fig. 3 are representative of the zircon populations. All zircon grains used for CL investigation and for dating purposes are prismatic with magmatic habit. From the CL photographs, it can be observed that most grains have two to three growth stages. Low CL intensity that is identified at the crystal margin of all grains from the metagranites and quartzites probably resulted from a common metamorphic overprint. On the other hand, different CL features can be observed in zircon grains from the two rock types. Magmatic zoning is better preserved in zircon grains from the metagranites, whereas zircons from the quartzites are more strongly overprinted by late event(s). Recrystallisation prior to the metamorphic overprint is commonly observed in zircon grains from the quartzites. Small xenocrystal domains can be observed in some grains of the metagranite TH-11.

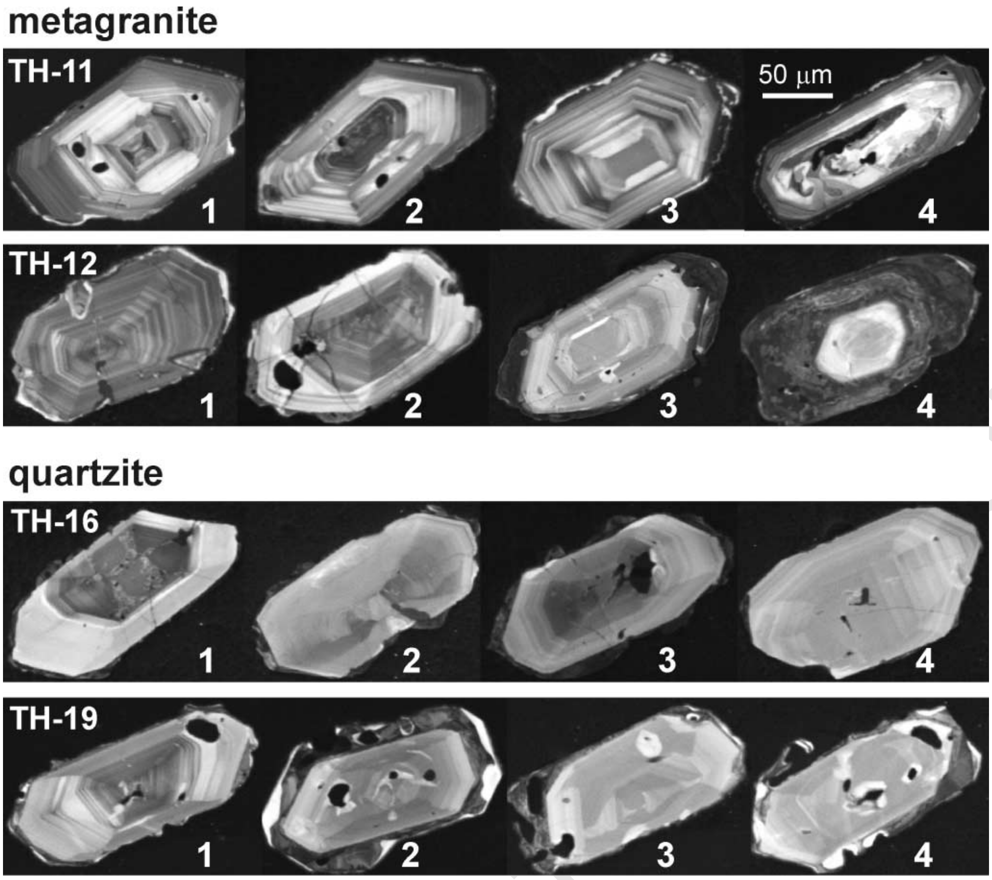

Fig. 3. CL photographs of zircon populations of metagranites (samples TH-11 and TH-12) and quartzites (samples TH-16 and TH-19). Metamorphic rims are commonly observed in all grains. Magmatic oscillatory zoning is better preserved in the grains from the metagranites. Intense recrystallisation can be observed in most of the grains from the quartzites.

The U–Pb analytical data are given in Table 2 and plotted in concordia diagrams (Figs. 4 and 5). All analysed zircon fractions (comprising up to three grains) from metagranites and quartzites give U–Pb ages with different degrees of discordance. Four of five fractions from metagranite TH-11 gave $^{207}Pb/^{206}Pb$ ages of between 730 and 770 Ma. The other one yielded an older $^{207}Pb/^{206}Pb$ age of 846 Ma, probably indicating that old inherited core was present in this fraction. This fraction distinctly has a low Th/U ratio (corresponding to low $^{208}Pb^{*}/^{206}Pb^{*}$ ratio of 0.11), probably suggesting a different origin from other analysed zircon fraction. A discordia line defined by the first four data points gives U–Pb intercept ages of $799+23/-18$ and $246+59/-62$ Ma. This lower-intercept model age is within the large error similar to the time of the collision between the South and North China Blocks, dated at about 230–220 Ma (e.g. Li et al., 1993; Ames et al., 1993, 1996; Eide et al., 1994; Hacker and Wang, 1995; Chavagnac et al., 2001). Assumed that the analysed zircons were subjected to Pb-loss simultaneously with the Early Mesozoic collision, the data points are calculated again using a forced regression through 220 ± 10 Ma, which approximately represents the collision time, and hence a more fixed upper-intercept model age of 791 ± 5 Ma can be obtained. Similarly, one of six zircon fractions from the metagranite TH-12 has a lower $^{208}Pb^{*}/^{206}PB^{*}$ ratio of 0.12 and an older $^{207}Pb/^{206}Pb$ age of 998 Ma, indicating the existence of an inherited core. The

Table 2
Zircon U–Pb analytical data of metagranites and quartzites from the Susong HP metamorphic zone

Sample	$^{206}Pb/^{204}Pb$	U (ppm)	Pb (ppm)	Pb* (ppm)	Atomic ratios				Apparent ages (Ma)		
					$^{208}Pb^*/^{206}Pb^*$	$^{206}Pb/^{*238}U$	$^{207}Pb^*/^{235}U$	$^{207}Pb^*/^{206}Pb^*$	$^{206}Pb^*/^{238}U$	$/^{207}Pb^*/^{235}U$	$^{207}Pb^*/^{206}Pb^*$
Metagranites											
TH-11											
(1) Big, thick, 1 gr	908	182	22.5	21.6	0.32	0.09961 ± 200	0.8747 ± 177	0.06369 ± 12	612	638	731
(2) Long, thick, 1 gr	696	135	17.0	16.1	0.26	0.10462 ± 212	0.9229 ± 188	0.06398 ± 17	641	664	741
(3) Long, thin, 2 grs	730	177	24.3	23.2	0.26	0.11435 ± 233	1.0237 ± 211	0.06492 ± 19	698	716	772
(4) Fine, short, 2 grs	215	147	22.0	17.7	0.24	0.10672 ± 218	0.9382 ± 208	0.06376 ± 52	654	672	734
(5) Fine, short, 2 grs	1079	115	12.1	11.7	0.11	0.10025 ± 204	0.9299 ± 192	0.06727 ± 20	616	668	846
TH-12											
(1) Big, thick, 1 gr	1120	336	32.8	31.6	0.20	0.08647 ± 174	0.7462 ± 151	0.06259 ± 12	535	566	694
(2) Long, thick, 1 gr	1277	235	25.3	24.6	0.22	0.09407 ± 189	0.8242 ± 166	0.06355 ± 10	580	610	727
(3) Fine, long, 3 grs	749	198	16.4	15.9	0.23	0.08026 ± 164	0.6878 ± 143	0.06216 ± 23	498	532	680
(4) Fine, short, 2 grs	814	185	13.8	13.5	0.19	0.06748 ± 158	0.5693 ± 135	0.06119 ± 20	421	458	646
(5) Short, thick, 1 gr	7209	470	35.8	35.7	0.12	0.07356 ± 148	0.7346 ± 146	0.07242 ± 5	458	559	998
(6) Long, 2 grs	1546	230	21.3	20.6	0.21	0.08188 ± 164	0.7024 ± 142	0.06222 ± 8	507	540	682
Quartzites											
TH-15											
(1) Small, short, 2 grs	1575	186	10.3	10.1	0.16	0.05189 ± 105	0.4100 ± 83	0.05730 ± 16	326	349	503
(2) Fine, long, 2 grs	1016	120	8.1	7.8	0.24	0.05817 ± 121	0.4688 ± 99	0.05845 ± 23	365	390	547
(3) Short, 1 gr	2653	197	12.8	12.7	0.24	0.05794 ± 117	0.4738 ± 98	0.05931 ± 27	363	393	579
(4) Long, 2 grs	2110	193	11.8	11.7	0.24	0.05478 ± 111	0.4341 ± 88	0.05747 ± 16	344	366	510

Table 2 (*Continued*)

					Atomic ratios				Apparent ages (Ma)		
(5) Long, 1 gr	1380	212	13.7	13.5	0.25	0.05639 ± 114	0.4478 ± 91	0.05759 ± 12	354	376	514
TH-16											
(1) Thick, short, 1 gr	1199	627	68.4	65.5	0.20	0.09597 ± 243	0.8389 ± 213	0.06339 ± 15	591	619	722
(2) Thick, short, 1, gr	1250	668	70.6	67.7	0.20	0.09316 ± 188	0.8140 ± 167	0.06336 ± 15	574	605	721
(3) Long, 2 grs	637	689	62.9	57.9	0.19	0.07806 ± 168	0.6758 ± 147	0.06279 ± 23	485	524	701
(4) Long, 1 gr	1216	752	87.7	84.0	0.18	0.10407 ± 220	0.9049 ± 193	0.06306 ± 11	638	654	710
(5) Small, short, 3 grs	646	450	36.3	33.5	0.19	0.06909 ± 158	0.5971 ± 139	0.06267 ± 26	431	475	697
(6) Small, long, 2 grs	966	424	34.3	32.6	0.17	0.07239 ± 170	0.6190 ± 146	0.06201 ± 18	451	489	675
TH-19											
(1) Short, 1 gr	456	254	14.8	13.2	0.14	0.05030 ± 109	0.3931 ± 95	0.05668 ± 57	316	337	479
(2) Long, 1 gr	370	248	13.6	11.9	0.15	0.04632 ± 100	0.3529 ± 80	0.05525 ± 33	292	307	423
(3) Long, 2 grs	1649	211	11.5	11.3	0.15	0.05147 ± 104	0.4098 ± 84	0.05774 ± 20	324	349	520
(4) Fine, long, 3 grs	1886	218	10.1	10.0	0.13	0.04533 ± 92	0.3478 ± 71	0.05565 ± 11	286	303	439
(5) Fine, short, 2 grs	1986	199	10.8	10.7	0.19	0.05030 ± 105	0.3956 ± 80	0.05704 ± 13	316	338	493
(6) Thin, long, 2 grs	1863	180	9.2	9.1	0.15	0.04923 ± 99	0.3866 ± 80	0.05696 ± 20	310	332	490

Errors are given as $2\sigma_m$. gr, grain; grs, grains. Concentrations of U and Pb are calculated with estimated zircon weights. The $^{206}Pb/^{204}Pb$ ratios are measured values. Row analytical data were calculated with the 'Pbdat' program Ludwig (1988).

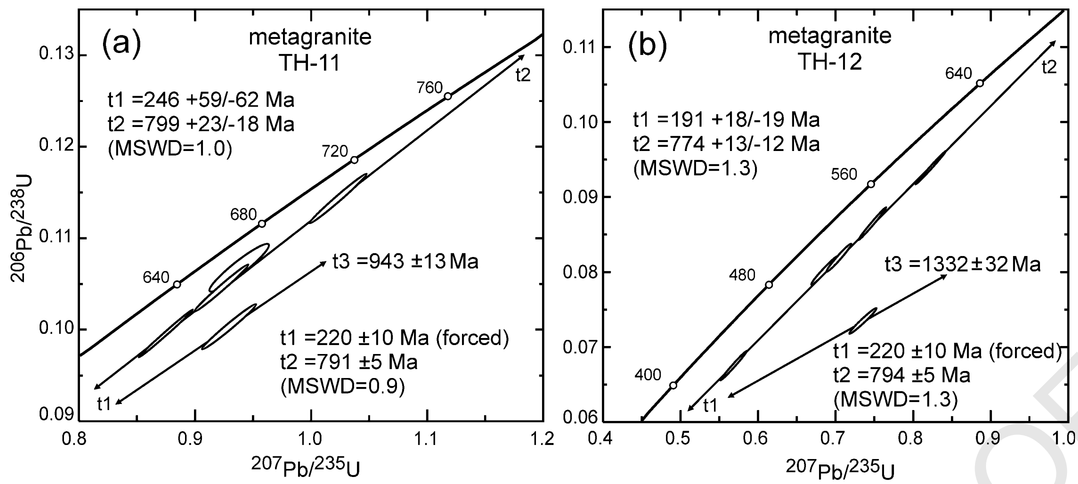

Fig. 4. Zircon U–Pb concordia diagram; (a) metagranite TH-11 and (b) metagranite TH-12.

other five fractions have $^{207}Pb/^{206}Pb$ ages between 646 and 727 Ma and define a discordia that gives intercept ages of 774+13/−12 and 191+18/−19 Ma. When the forced regression through 220±10 Ma is also applied to these data, similar to the method for sample TH-11, an upper-intercept age of 794±5 Ma is obtained. These two zircon fractions containing inherited cores give upper-intercept model ages of 943±13 and 1332±32 Ma (Fig. 4), when a forced regression through 220±10 Ma is considered.

Analyses of seventeen zircon fractions were performed on three quartzites (samples TH-15, TH-16 and TH-19). All of them unexpectedly give young $^{207}Pb/^{206}Pb$ ages between 422 and 722 Ma, similar to those of the metagranites. Zircon fractions from samples TH-15 and TH-19 yielded more discordant U–Pb ages than those from sample TH-16 and regressions of these data give less precise upper-intercept ages. Five data points of sample TH-15 define a discordia giving intercept ages of 826+95/−85 and 238+22/−29 Ma (Fig. 5a). The discordia regressed through six data points of sample TH-19 yields intercept ages of 863+93/−86 and 229+13/−17 Ma (Fig. 5b). When the regression is forced through 220±10 Ma, the data of the two samples yield upper-intercept ages of 773+23/−22 and 820±21 Ma, respectively. Six zircon fractions of sample TH-16 define a discordia with intercept ages of 727±4 and 72±14 Ma (Fig. 5c). When forced regression through 220 Ma is applied, the data give an upper-intercept age of 794±5 Ma. This age is similar to the $^{207}Pb/^{206}Pb$ evaporation ages obtained from two zircon grains (Fig. 5d; Table 3). Two other grains from the same sample give younger $^{207}Pb/^{206}Pb$ evaporation ages of 750±24 and 730±20 Ma, probably indicating an influence of later metamorphic overprint.

4.4. Nd isotopic composition

The Nd isotopic compositions of seven samples are given in Table 1. Nd model ages (T_{DM}) are calculated using a two-stage model, following the approach of Liew and Hofmann (1988). Two metagranite samples have model ages of 2.3–2.4 Ga, whereas five quartzite samples have younger model ages between 1.9 and 2.2 Ga. These results are similar to the data formerly reported from the Dabie Mountains (Ma et al., 2000) and generally fall in the T_{DM} range of sedimentary rocks from the northwestern Yangtze Block as well (Chen and Jahn, 1998). Initial ε_{Nd}-values of two metagranites calculated back to 780 Ma are −12.4 and −11.1, which are slightly lower than the ε_{Nd}-values of five quartzite samples that range from −9.7 to −6.0, when also calculated back to 780 Ma for a comparison.

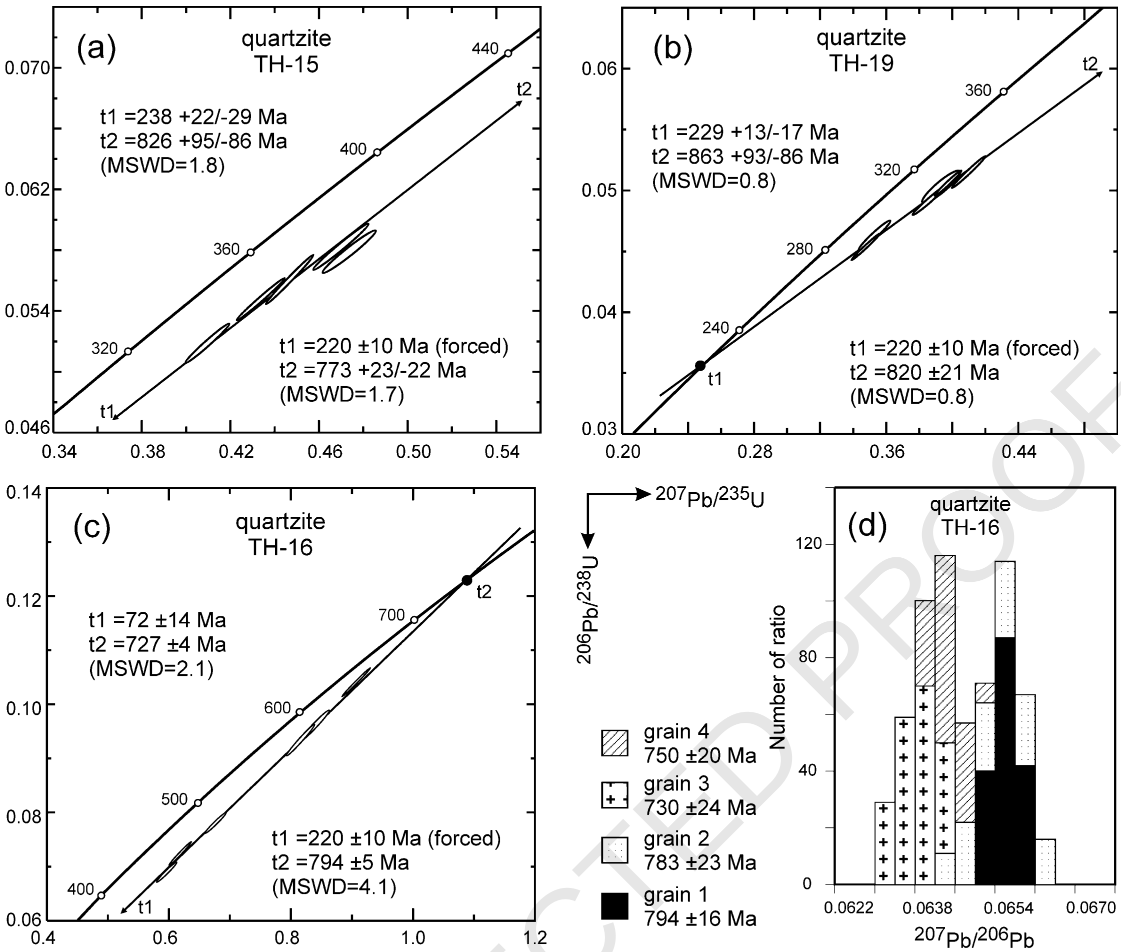

Fig. 5. Zircon U–Pb concordia diagram and $^{207}Pb/^{206}Pb$ histogram; (a) quartzite TH-15, (b) quartzite TH-19, and (c) and (d) quartzite TH-16.

Table 3
Single zircon evaporation data of quartzite TH-16

Grain	Number of ratios	Mean $^{207}Pb/^{206}Pb$ value ($2\sigma_m$)	$^{207}Pb/^{206}Pb$ age (Ma)
1	169	0.06560 ± 51	794 ± 16
2	130	0.06526 ± 72	783 ± 23
3	210	0.06366 ± 72	730 ± 24
4	144	0.06425 ± 61	750 ± 20

5. Discussion

5.1. Origin of the metagranites

Both the metagranites and quartzites have analogous Nd isotopic compositions (ε_{Nd}-value and T_{DM}) to the metasedimentary rocks from the Yangtze Block (Chen and Jahn, 1998), consistent with a commonly shared opinion that the Susong HP metamorphic zone is part of this block. The metagranites have lower initial ε_{Nd}-values (-12.4 to -11.1), compared with the quartzites (-9.7 to -6.0), probably indicating a predominant crustal material origin. The characteristics of trace element and REE contents of both quartzites and metagranites are comparable with those of average shales (e.g. Nance and Taylor, 1976). The quartzites but are different from the metagranites further in REE-contents, especially in LREE-concentrations. These differences in trace element and Nd isotopic compositions between the metagranites and quartzites do not favour that protoliths of the metagranites originated exclusively from sedimentary rocks, whose isotopic and geochemical characteristics are represented e.g. by the quartzites. They must have been produced partly from an older crustal component underneath, if a component similar to the quartzites was involved into the granite formation.

The metagranites display fractionation between LREEs and HREEs, but low Gd_N/Yb_N ratios suggest that the fractionation of HREE-bearing mineral phases, e.g. garnet and amphibole, was of minor importance in the source. This feature implies that the melts were formed at shallow crustal levels where such mineral phases are unstable, in contrast to many granitoids that originate from a thickened crust in a convergent or collisional setting. Such granitoids often have a highly fractionated HREE composition (high Gd_N/Yb_N value), due to the presence of garnet and/or amphibole in the sources at HPs (e.g. Kay et al., 1994; Kay and Abbruzzi, 1996).

5.2. Late Proterozoic magmatism

The U–Pb zircon age data of the metagranites and quartzites in this study are the first ones

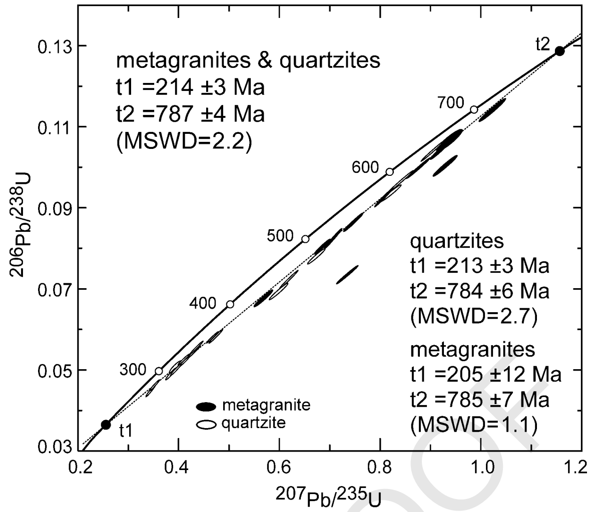

Fig. 6. A compilation of zircon U–Pb ages from the metagranites and quartzites shown in a concordia diagram. Data are the same as shown in Fig. 4 and Fig. 5. Except for two zircon fractions containing inherited radiogenic Pb, regression of all analytical data of the metagranites and quartzites defines a discordia line (MSWD = 2.2) with intercept ages of 787 ± 4 Ma and 214 ± 3 Ma. When data of two rock types are separately regressed, similar upper- and lower-intercept ages are derived, i.e. 784 ± 6 Ma and 213 ± 3 Ma for the quartzites (MSWD = 2.7) and 785 ± 7 Ma and 205 ± 12 Ma for the metagranites (MSWD = 1.1).

reported for the northern part of the Susong HP metamorphic zone. The U–Pb upper-intercept ages of zircons from two different rock types, two metagranites and three quartzites, are constrained at around 770–790 Ma, especially when forced regressions through 220 ± 10 Ma are considered. A distribution of all data in a concordia diagram is shown in Fig. 6. From this data array, it can be observed that all analysed zircon fractions, except for two of the metagranites, which obviously contain an inherited radiogenic Pb component, define the same discordia trend. Zircons from the two metagranites occupy the upper part of the array, whereas zircons from the quartzites mainly inhabit the lower part. This feature can be explained as different responses of zircons from different rock types to the metamorphic overprint of about 220 Ma. Zircons from the quartzites underwent a more extensive Pb-loss, probably resulting from higher fluid activities that facilitated metamictisation of zircon crystals and subsequently led to radiogenic Pb-loss (e.g. Nasdala et al., 1995). The data array defines a discordia with intercept ages of 787±4 and 214±3 Ma, respectively. Separate regressions of the data sets from the metagranites and quartzites yield similar model ages, especially the identical upper-intercept ages (Fig. 6).

The lower-intercept age of 214 Ma is slightly younger than the UHP metamorphism (~230–220 Ma) that represents the collision between the Yangtze (South China) and North China Blocks (e.g. Ames et al., 1993; Li et al., 1993, 2000; Chavagnac and Jahn, 1996; Chavagnac et al., 2001; Rowley et al., 1997; Hacker et al., 1998; Webb et al., 1999). Nevertheless, the 214 Ma age is coincidental to the time of an early exhumation of the UHP metamorphic rocks (e.g. Nie et al., 1994; Webb et al., 1999; Hacker et al., 1998; Xu et al., 2000). Thus, the 214 Ma age can either represent the timing of a late HP metamorphism or the exhumation of UHP–HP metamorphic rocks.

As demonstrated by the CL photographs, the oscillatory zoning of magmatic origin is well preserved in most zircon grains from the metagranites and it can be concluded that the 785±7 Ma upper-intercept age, defined by the two metagranites (Fig. 6), likely represents the crystallisation time. The Late Proterozoic crystallisation age of the metagranites is similar to those of eclogites and orthogneisses in the South Dabie UHP metamorphic zone (e.g. Ames et al., 1993; Rowley et al., 1997), in the North Dabie gneiss zone (e.g. Xue et al., 1997; Hacker et al., 1998), and in the Beihuaiyang low-grade zone (Hacker et al., 1998). However, many of the reported upper-intercept ages have large uncertainties and range from about 650–850 Ma. Similar ages have also been reported from the northern margin of the Yangtze Block (e.g. Kröner et al., 1993; Xue et al., 1996). They are commonly interpreted as crystallisation ages of the precursor rocks. The precursors of some eclogites from the South Dabie UHP metamorphic zone were interpreted as magmatic products of a rift environment between about 700 and 800 Ma (e.g. Ames et al., 1996). Although there is no obvious evidence favouring an extension environment in the Dabie area during this time, several studies show that this break-up can be traced along the periphery of the Yangtze Block, e.g. there are bimodal volcanic rocks of ~800–820 Ma at the western margin (e.g. Li et al., 2001), maficultramafic dykes at the southern margin (e.g. Li et al., 1999), and mafic dyke swarms of about 800 Ma in the Wudan Mountains at the northern margin (e.g. Zhou et al., 1998). It is believed that the extension and break-up of the Yangtze Block took place shortly after its complete consolidation during the *Jinning* orogen between about 1000 and 850 Ma (e.g. Zhou et al., 1998) and after the formation of the Late Proterozoic supercontinent, Rodinia (e.g. Li et al., 1995). These magmatic activities could be related to the break-up of Rodinia during Late Proterozoic, if the Yangtze (South China) Block was once part of the supercontinent, as suggested by some researchers (e.g. Li et al., 1995; Li and Powell, 2001).

5.3. Late Proterozoic metamorphism

The rock sequences of the Susong HP metamorphic zone are considered to be Middle Proterozoic in age, but the dating results demonstrate that old ages of detrital zircons from all three analysed quartzites are completely absent. Both the upper-intercept model U–Pb ages and $^{207}Pb/^{206}Pb$ ages obtained by the evaporation method are similar to the crystallisation ages of the metagranites (Fig. 6). This phenomenon implies either a unique sedimentary source or a nearly complete resetting of zircon U–Pb system at around 780 Ma. The first possibility seems likely, only if the quartzites originated from in situ weathered Late Proterozoic magmatic rocks that crystallised simultaneously with the metagranites. The second possibility implies that Pb-loss from the zircons is probably related to metamorphism contemporaneous with the magmatism during Late Proterozoic.

An argument against Pb-loss is that the rate of Pb diffusion in zircon is extremely slow, as shown in several experimental studies (e.g. Lee et al., 1997a; Cherniak and Watson, 2000). The zircon U–Pb system is commonly believed to have a very high isotope closure temperature and theoretically cannot be reset during metamorphism and alteration at crustal levels, when only thermal diffusion is considered as a major factor. However, many examples show that Pb-loss is demonstrated in zircons not only from high-grade metamorphic rocks, but also from low-grade metamorphic or weathered rocks (e.g. Gebauer and Grünenfelder, 1976; Stern et al., 1966). It has been shown that Pb-loss can be largely accelerated by recrystallisation (e.g. Pidgeon, 1992; Pidgeon et al., 1998), metamictisation (e.g. Nasdala et al., 1995, 1996), crystal lattice damage (e.g. Davis and Krogh, 2000; Chen et al., in press), and especially fluid participation (e.g. Villa, 1997; Sinha et al., 1992). Thus, it is possible that old detrital zircons of the quartzites lost all radiogenic Pb, depending on metamorphic conditions e.g. temperature and fluid activity during the metamorphic overprint. Therefore, we favour that the zircon age pattern of the quartzites reflects a syn-magmatic-metamorphic event rather than a unique sedimentary source. This metamorphic event probably took place in a rifting tectonic environment along the periphery of the Yangtze Block. Deep crustal HT-LP regional metamorphism can be associated with extensional tectonics due to unusual heat flow (e.g. Wickham and Oxburgh, 1985), especially in crustal-penetrative detachment zones (Sandiford and Powell, 1986).

6. Conclusions

Zircon U–Pb ages and geochemical as well as Nd isotopic data, which are obtained on the metagranites and quartzites from the northern part of the Susong HP metamorphic zone, permit some preliminary conclusions on the evolution of this zone prior to the collision between the North and South China blocks.

Protoliths of the metagranites originated from melting of a Yangtze (South China) crustal section at around 780 Ma. Identical U–Pb intercept ages obtained from both metagranites and quartzites not only suggest a common metamorphic overprint related to the collision during Early Mesozoic, but also indicate a thermal activity at around 780 Ma. This Late Proterozoic event probably represents simultaneous metamorphism and magmatism within a rift setting along the periphery of the Yangtze Block. The fact that old detrital zircons are completely absent in the quartzites probably indicates resetting of the zircon U–Pb system during this event.

Acknowledgements

Sincere thanks are due to B.-M. Jahn, V. Chavagnac, and A. Kröner for crucial comments and suggestions to improve the manuscript. We thank H. Fan, Q. Qiang, and X. Zhang for discussion and help during the fieldwork, G. Markl for access to the microprobe for cathodoluminescence analysis, and M. Schumann and G. Bartholomä for XRF analysis. This study was funded by the National Priority Research and Development Program of China (G1999075502) and resulted from the cooperative project between Chinese Academy of Sciences and University of Tübingen.

References

Ames, L., Tilton, G.R., Zhou, G.-Z., 1993. Timing of collision of the Sino-Korean and Yangtze Cratons: U–Pb zircon dating of coesite-bearing eclogites. Geology 21, 339–342.

Ames, L., Zhou, G.-Z., Xiong, B.-C., 1996. Geochronology and isotopic character of ultrahigh pressure metamorphism with implications for collision of the Sino-Korean and Yangtze cartons, central China. Tectonics 15, 472–489.

Anhui Geological Survey (AGS), 1999. Explanation of the geological map (1:250 000) of the Dabie Mountains within Anhui Province. Anhui Geological Survey, Hefei, pp. 1–44 (in Chinese).

Carswell, D.A., O'Brien, P.J., Wilson, R.N., Zhai, M., 1997. Thermobarometry of phengite-bearing eclogites in the Dabie Mountains of central China. J. Metamorph. Geol. 15, 239–252.

Chavagnac, V., Jahn, B.-M., 1996. Coesite-bearing eclogites from the Bixiling Complex, Dabie Mountains, China: Sm–Nd ages, geochemical characteristics and tectonic implications. Chem. Geol. 133, 29–51.

Chavagnac, V., Jahn, B.-M., Villa, I.M., Whitehouse, M.J., Liu, D., 2001. Multichronometric evidence for an in situ origin of the ultrahigh-pressure metamorphic terrane of Dabieshan. China J. Geol. 109, 633–646.

Chen, F., Hegner, E., Todt, W., 2000. Zircon ages and Nd isotopic and chemical compositions of orthogneisses from the Black forest, Germany: evidence for a Cambrian magmatic arc. Int. J. Earth Sci. 88, 791–802.

Chen, F., Siebel, W., Satir, M. Zircon U–Pb and Pb-isotope fractionation during stepwise HF-acid leaching and geochronological implications. Chem. Geol., in press.

Chen, F., Siebel, W., Satir, M., Terzioglu, N., Saka, K., 2002. Late Proterozoic continental accretion in the northwestern Turkey: evidence from zircon U–Pb and Pb–Pb dating and Nd–Sr isotopes. Int. J. Earth Sci. 91, 469–481.

Chen, J., Jahn, B.-M., 1998. Crustal evolution of southeastern China: Nd and Sr isotopic evidence. Tectonophysics 284, 101–133.

Cherniak, D.J., Watson, E.B., 2000. Pb diffusion in zircon. Chem. Geol. 172, 5–24.

Cocherie, A., Guerrot, C., Rossi, P.H., 1992. Single-zircon dating by step-wise Pb evaporation: comparison with other geochronological techniques applied to the Hercynian granites of Corsica, France. Chem. Geol. 101, 131–141.

Cong, B.-L., Zhai, M.-G., Carswell, D.A., Wilson, R.N., Wang, Q.-C., Zhao, Z., Windley, B.F., 1995. Petrogenesis of ultrahigh-pressure rocks and their country rocks at Shuanghe in Dabieshan, central China. Eur. J. Mineral. 7, 119–138.

Davis, D.W., Krogh, T.E., 2000. Preferential dissolution of 234U and radiogenic Pb from α-recoil-damaged lattice sites in zircon: implications for thermal histories and Pb isotopic fractionation in the near surface environment. Chem. Geol. 172, 41–58.

Dong, S.-W., Chen, J.-F., Huang, D.-Z., 1998. Differential exhumation of tectonic units and ultrahigh-pressure metamorphic rocks in the Dabie terrain, China. Island Arc 7, 173–185.

Eide, E.A., McWilliams, M.O., Liou, J.G., 1994. $^{40}Ar/^{39}Ar$ geochronology and exhumation of high-pressure to ultrahigh-pressure metamorphic rocks in east-central China. Geology 22, 601–604.

Enkin, R.J., Courtillot, V., Leloup, Ph., Yang, Z., Zhang, J., Zhuang, Z., 1992. The palaeomagnetic record of uppermost Permian, lower Triassic rocks from the south China block. Geophys. Res. Lett. 19, 2147–2150.

Gebauer, D., Grünenfelder, M., 1976. U–Pb zircon and Rb–Sr whole rock dating of low-grade metasediments, example: Montagne Noir (Southern France). Contrib. Mineral. Petrol. 59, 13–32.

Hacker, B.R., Ratschbacher, L., Webb, L., Dong, S.-W., 1995. What brought them up? Exhumation of the Dabie Shan ultrahigh-pressure rocks. Geology 23, 743–746.

Hacker, B.R., Ratschbacher, L., Webb, L., Ireland, T., Walker, D., Dong, S.-W., 1998. U/Pb zircon ages constrain the architecture of the ultrahigh-pressure Qinling–Dabie orogen, China. Earth Planet Sci. Lett. 161, 215–230.

Hacker, B.R., Wang, Q.-C., 1995. Ar/Ar geochronology of ultrahigh-pressure metamorphism in central China. Tectonics 14, 994–1006.

Hanchar, J.M., Miller, C.F., 1993. Zircon zonation patterns as revealed by cathodoluminescence and backscattered electron images: implications for interpretation of complex crustal histories. Chem. Geol. 110, 1–13.

Hsü, K.J., Wang, Q., Li, J., Zhou, D., Sun, S., 1987. Tectonic evolution of Qinling Mountains, China. Ecolog. Geol. Helv. 80, 735–752.

Huang, W., Wu, Z.W., 1992. Evolution of the Qinling orogenic belt. Tectonics 11, 371–380.

Jenner, G.A., Longerich, H.P., Jackson, S.E., Fryer, B.J., 1990. ICP-MS—a powerful new tool for high precision trace element analysis in earth sciences: evidence from analysis of selected USGS standards. Chem. Geol. 83, 133–148.

Kay, S.M., Abbruzzi, J.M., 1996. Magmatic evidence for Neogene lithospheric evolution of the central Andean 'flat-slab' between 30°S and 32°S. Tectonophysics 259, 15–28.

Kay, S.M., Coira, B., Viramonte, J., 1994. Young mafic back arc volcanic rocks as indicators of continental lithospheric delamination beneath the Argentine Puna plateau, central Andes. J. Geophys. Res. 99 (B12), 24323–24339.

Klimetz, M.P., 1983. Speculations on the Mesozoic plate tectonic evolution of eastern China. Teconics 2, 139–166.

Kober, B., 1986. Whole-grain evaporation for $^{207}Pb/^{206}Pb$ age investigations on single zircons using a double-filament thermal ion source. Contrib. Mineral. Petrol. 93, 481–490.

Krogh, T.E., 1982. Improved accuracy of U–Pb zircon ages by the creation of more concordant systems using an air abrasion technique. Geochim. Cosmochim. Acta 46, 637–649.

Kröner, A., Zhang, G.-W., Sun, Y., 1993. Granulites in the Tongbai area, Qinling belt, China: geochemistry, petrology, single zircon geochronology, and implications for the tectonic evolution of eastern Asia. Tectonics 12, 245–255.

Lee, J.K.W., Williams, I.S., Ellis, D.J., 1997a. Pb, U and Th diffusion in natural zircon. Nature 390, 159–161.

Lee, Y.S., Nishimura, S., Min, K.D., 1997b. Paleomagnetotectonics of East Asia in the Proto-Tethys Ocean. Tectonophysics 270, 157–166.

LeMaitre, R.W., 1989. A Classification of Igneous Rocks and Glossary of Terms. Blackwell, Oxford, pp. 1–193.

Lerch, M.F., Xue, F., Kröner, A., Zhang, G.W., Todt, W., 1995. A Middle Silurian–Early Devonian magmatic arc in the Qinling Mountains of central China. J. Geol. 103, 437–449.

Li, S.-G., Jagoutz, E., Chen, Y.-Z., Li, Q.-L., 2000. Sm–Nd and Rb–Sr isotopic chronology and cooling history of ultrahigh pressure metamorphic rocks and their country rocks at Shuanghe in the Dabie terrain, central China. Geochim. Cosmochim. Acta 64, 1077–1093.

Li, S.-G., Xiao, Y.-L., Liou, D.-L., Chen, Y.-Z., Ge, N.-J., Zhang, Z.-Q., Sun, S.-S., Cong, B.-L., Zhang, R.-Y., Hart, S.R., Wang, S.-S., 1993. Collision of the North China and Yangtze Blocks and formation of coesite-bearing eclogites: timing and processes. Chem. Geol. 109, 89–111.

Li, X.-H., Li, Z.X., Zhou, H., Liu, Y., Kinny, P.D., 2001. U–Pb zircon geochronology, geochemistry and Nd isotopic study of Neoproterozoic bimodal volcanic rocks in the

Kangdian Rift of South China: implications for the initial rifting of Rodinia. Precambrian Res. 113, 135–155.

Li, Z.-X., Li, X.-H., Kinny, P.D., 1999. The breakup of Rodinia: did it start with a mantle plume beneath South China? Earth Planet Sci. Lett. 173, 171–181.

Li, Z.-X., Powell, C.McA., 2001. Anoutline of the palaeogeographic evolution of the Australasian region since the beginning of the Neoproterozoic. Earth Sci. Rev. 53, 237–277.

Li, Z.-X., Zhang, L., Powell, C.McA., 1995. South China in Rodinia: part of the missing link between Australia—East Antarctica and Laurentia? Geology 23, 407–410.

Liew, T.C., Hofmann, A.W., 1988. Precambrian crustal components, plutonic associations, plate environment of the Hercynian fold belt of central Europe: indications from a Nd and Sr isotopic study. Contrib. Mineral. Petrol. 98, 129–138.

Liou, J.-G., Wang, Q.-C., Zhai, M.-G., Zhang, R.-Y., Cong, B.-L., 1995. Ultrahigh-P metamorphic rocks and their associated lithologies from the Dabie terrain, Central China: A field trip guide to the Third international eclogite field symposium. Chinese Sci. Bull. 40 (Suppl.), 1–40.

Liu, X., Hao, J., 1989. Structure and tectonic evolution of the Tongbai-Dabie range in the East Qiling collisional belt, China. Tectonics 8, 637–645.

Ludwig, K.R., 1988. Pbdat for MS-Dos—a computer program for IBM-PC compatibles for processing raw Pb–U–Th isotope data. Open-file Report 88–542, US Geol. Surv., 1–37.

Ma, C.-Q., Ehlers, C., Xu, C., Li, Z., Yang, K., 2000. The roots of the Dabieshan ultrahigh-pressure metamorphic terrane; constraints from geochemistry and Nd–Sr isotope systematics. Precambrian Res. 102, 279–301.

Ma, C.-Q., Li, Z., Ehlers, C., Yang, K., Wang, R., 1998. A post-collisional magmatic plumbing system; Mesozoic granitoid plutons from the Dabieshan high-pressure and ultrahigh-pressure metamorphic zone, east-central China. Lithos 45, 431–456.

Ma, W., 1989. Tectonics of the Tongbai-Dabie fold belt. J. SE. Asian Sci. 3, 77–85.

Mattauer, M., Matte, Ph., Malavieille, J., Tapponnier, P., Maluski, H., Xu, Z., Lu, Y., Tang, Y., 1985. Tectonics of the Qinling belt: build-up and evolution of eastern Asia. Nature 317, 496–500.

Mattauer, M., Matte, Ph., Maluski, H., Xu, Z.-Q., Zhang, Q.-W., Wang, Y.-M., 1991. Palaeozoic and Triassic plate boundary between North and South China: new structural and radiometric data on the Dabie-Shan (Eastern China). C. R. Acad. Sci. Paris (Ser. II) 312, 1227–1233.

McLennan, S.M., 1989. Rare earth elements in sedimentary rocks: influence of provenance and sedimentary processes. In: Lipin, B.R., McKay, G.A. (Eds.), Geochemistry and Mineralogy of Rare Earth Elements. Reviews in Mineralogy, pp. 169–200.

Meng, Q.-R., Zhang, G.-W., 2000. Geologic framework and tectonic evolution of the Qinling orogen, central China. Tectonophysics 323, 183–196.

Nance, W.B., Taylor, S.R., 1976. Rare earth element pattern and crustal evolution I. Australian post-Archean sedimentary rocks. Geochim. Cosmochim. Acta 40, 1539–1551.

Nasdala, L., Irmer, G., Wolf, D., 1995. The degree of metamictization in zircon; a Raman spectroscopic study. Eur. J. Mineral. 7, 471–478.

Nasdala, L., Pidgeon, R.T., Wolf, D., 1996. Heterogeneous metamictization of zircon on a microscale. Geochim. Cosmochim. Acta 60, 1091–1097.

Nie, S., Yin, A., Rowley, D.B., Jin, Y., 1994. Exhumation of the Dabie Shan ultrahigh-pressure rocks and accumulation of the Songpan-Ganzi flysch sequence, central China. Geology 22, 999–1002.

Okay, A.I., 1993. Petrology of a diamond and coesite-bearing metamorphic terrain: Dabie Shan, China. Eur. J. Mineral. 5, 659–673.

Parrish, R.R., 1987. An improved micro-capsule for zircon dissolution in U–Pb geochronology. Chem. Geol. 66, 99–102.

Pidgeon, R.T., 1992. Recrystallization of oscillatory-zoned zircon: some geochronological and petrological implications. Contrib. Mineral. Petrol. 110, 463–472.

Pidgeon, R.T., Nemchin, A.A., Hitchen, G.J., 1998. Internal structures of zircons from Archaean granites from the Darling Range Batholith; implications for zircon stability and the interpretation of zircon U–Pb ages. Contrib. Mineral. Petrol. 132, 288–299.

Roddick, J.C., Sullivan, R.W., Dudás, F.Ö., 1992. Precise calibration of Nd tracer isotopic composition for Sm–Nd studies. Chem. Geol. 97, 1–8.

Rowley, D.B., Xue, F., Tucker, R.D., Peng, Z.-X., Baker, J., Davis, A., 1997. Ages of ultrahigh pressure metamorphism and protolith orthogneisses from the eastern Dabie Shan: U/Pb zircon geochronology. Earth Planet Sci. Lett. 151, 191–203.

Sandiford, M., Powell, R., 1986. Deep crustal metamorphism during continental extension: modern and ancient examples. Earth Planet Sci. Lett. 79, 151–158.

Sang, B., Chen, Y., Shao, G., 1987. Rb–Sr ages of metamorphic series of the Susong Group at southeastern foot of the Dabie Mountains, Anhui Province, and their tectonic significance. Reg. Geol. China 4, 364–370 (in Chinese).

Sinha, A.K., Wayne, D.M., Hewitt, D.A., 1992. The hydrothermal stability of zircon; preliminary experimental and isotopic studies. Geochim. Cosmochim. Acta 56, 3551–3560.

Stacey, J.S., Kramers, J.D., 1975. Approximation of terrestrial lead isotope evolution by a two stage model. Earth Planet Sci. Lett. 26, 207–221.

Stern, T.W., Goldich, S.S., Newel, M.F., 1966. Effect of weathering on the U–Pb zircon ages from the Morton gneiss, Minnesota. Earth Planet Sci. Lett. 1, 369–378.

Sun, S.S., 1982. Chemical composition and origin of the Earth's primitive mantle. Geochim. Cosmochim. Acta 46, 179–192.

Taylor, S.R., McLennan, S.M., 1985. The Continental Crust: its Composition and Evolution. Blackwell, Oxford.

Villa, I.M., 1997. Isotopic closure. Terra Nova 10, 42–47.

Webb, L.E., Hacker, B.R., Ratschbacher, L., McWilliams, M.O., Dong, S.-W., 1999. Thermochronologic constraints on deformation and cooling history of high- and ultrahigh-pressure rocks in the Qinling–Dabie orogen, eastern China. Tectonics 18, 621–638.

Wendt, I., 1986. Radiometrische Methoden in der Geochronologie. In: Clausthaler Tektonische Hefte, vol. 23. Pilger Verlag, p. 170.

Wickham, S., Oxburgh, E.R., 1985. Continental rifts as a setting for regional metamorphism. Nature 318, 330–333.

Wiedenbeck, M., Allé, P., Corfu, F., Griffin, W.L., Meier, M., Oberli, F., von Quadt, A., Roddick, J.C., Spiegel, W., 1995. Three natural zircon standards for U–Th–Pb, Lu–Hf, trace element and REE analyses. Geostand. Newslett. 19, 1–23.

Xie, Z., Chen, J.-F., Zheng, Y.-F., Zhang, X., Li, H.-M., Zhou, T.-X., 2001. Zircon U–Pb dating of the metamorphic rocks of different grades from the southern part of the Dabie Terrain in China. Phys. Chem. Earth 26, 685–693.

Xu, B., Grove, M., Wang, C., Zhang, L., Liu, S., 2000. $^{40}Ar/^{39}Ar$ thermochronology from the northwestern Dabie Shan: constraints on the evolution of Qinling–Dabie orogenic orogenic belt, east-central China. Tectonophysics 322, 279–301.

Xue, F., Kröner, A., Reischmann, T., Lerch, F., 1996. Palaeozoic pre- and post-collision calc-alkaline magmatism in the Qinling orogenic belt, central China, as documented by zircon ages on granitoid rocks. J. Geol. Soc. Lond. 153, 409–417.

Xue, F., Rowley, D.B., Tucker, R.D., 1997. U–Pb zircon ages of granitoid rocks in the North Dabie complex, eastern Dabie Shan, China. J. Geol. 105, 744–753.

Yin, A., Nie, S., 1993. An indentation model for the North and South China collision and the development of the Tan-Lu and Honam fault systems, eastern Asia. Tectonics 12, 801–813.

Zhai, X., Day, H.W., Hacker, B.R., You, Z., 1998. Paleozoic metamorphism in the Qinling orogen, Tongbai Mountains, central China. Geology 26, 371–374.

Zhai, M., Cong, B., Wang, Q., 1995. Susong metamorphic complex in Dabieshan, central China: a mobilized sedimentary cover of the Yangtze southern continental margin. Chin. Sci. Bull. 40 (Suppl.), 163–164.

Zhang, K.-J., 1997. North and South China collision along the eastern and southern North China margins. Tectonophysics 270, 145–156.

Zhou, D.-W., Zhang, C., Liu, L., Wang, J., 1998. Sm–Nd dating of basic dykes from the Wudang Block and a discussion of related problems. Acta Geosci. Sinica 19, 25–30 (in Chinese).